

# ATOMIC OXYGEN (ATOX) SIMULATION OF TEFLON FEP AND KAPTON H SURFACES USING A HIGH INTENSITY, LOW ENERGY, MASS SELECTED, ION BEAM FACILITY

R. Vered, E. Grossman, G.D. Lempert and Y. Lifshitz  
SOREQ NRC, Yavne 81800, Israel

## Abstract

A high intensity ( $> 10^{15}$  ions/cm<sup>2</sup>) low energy (down to 5 eV) mass selected ion beam (MSIB) facility was used to study the effects of ATOX on two polymers commonly used for space applications (Kapton H and Teflon FEP). The polymers were exposed to O<sup>+</sup> and Ne<sup>+</sup> fluences of  $10^{15}$  -  $10^{19}$  ions/cm<sup>2</sup>, using 30eV ions. A variety of analytical methods were used to analyze the eroded surfaces including: (i) atomic force microscopy (AFM) for morphology measurements (ii) total mass loss measurements using a microbalance, (iii) surface chemical composition using X-ray photoelectron spectroscopy (XPS), (iv) residual gas analysis (RGA) of the released gases during bombardment.

The relative significance of the collisional and chemical degradation processes was evaluated by comparing the effects of Ne<sup>+</sup> and O<sup>+</sup> bombardment. For 30 eV ions it was found that the Kapton is eroded via chemical mechanisms while Teflon FEP is eroded via collisional mechanisms.

AFM analysis was found very powerful in revealing the evolution of the damage from its initial atomic scale (roughness of ~ 1 nm) to its final microscopic scale (roughness  $> 1 \mu\text{m}$ ). Both the surface morphology and the average roughness of the bombarded surfaces (averaged over  $1 \mu\text{m} \times 1 \mu\text{m}$  images by the system's computer) were determined for each sample. For 30 eV a non linear increase of the Kapton roughness with the O<sup>+</sup> fluence was discovered (a slow increase rate for fluences  $\Phi < 5 \times 10^{17}$  O<sup>+</sup>/cm<sup>2</sup>, and a rapid increase rate for  $\Phi > 5 \times 10^{17}$  O<sup>+</sup>/cm<sup>2</sup>).

Comparative studies on the same materials exposed to RF and DC oxygen plasmas indicate that the specific details of the erosion depend on the simulation facility emphasizing the advantages of the ion beam facility.

## 1. Introduction

Erosion of surfaces by atomic oxygen (ATOX) has been the subject of many investigations in the past ten years<sup>(1-3)</sup>. It is now very well established that external surfaces of space systems orbiting with a velocity of 8 km/sec in low earth orbits (LEO) collide with the residual oxygen atoms at an effective energy of ~3-7eV and a flux of  $10^{14}$ - $10^{15}$  O/cm<sup>2</sup> sec. Flight

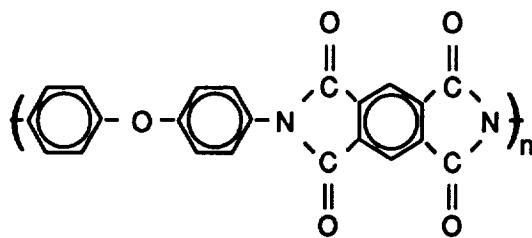
experiments have demonstrated that most organic surfaces are severely eroded by this exposure<sup>(1-6)</sup>. The ATOX problem initiated many studies of surface erosion by oxygen applying a variety of ground exposure facilities<sup>(7-13)</sup>. The complex nature of most of these systems in terms of a wide energy range and a mixture of species imposes severe difficulties in understanding the atomic oxygen erosion mechanisms and in establishing reliable ground simulation experiments for space applications. Contradictory models were proposed to explain the energy dependence of the degradation efficiency of Kapton<sup>(2,14)</sup>.

The present work describes studies performed using a unique mass selected ion beam facility capable of providing a high  $O^+$  flux and medium and low (5eV-45keV) energy. In this facility most of the relevant physical parameters (ion nature, flux, energy) can be controlled and varied. Two other less sophisticated systems, commonly used for ATOX simulation, RF plasma ("plasma asher") and DC plasma were also used for comparative studies. The present work is focused on ATOX effects in two commonly used polymers (Kapton H and Teflon FEP) by atomic oxygen. The work also demonstrates the possibilities offered by atomic force microscopy (AFM) for ATOX erosion studies detecting the erosion from the initial stage (nm scale) to the final stage ( $\mu m$  scale). Other diagnostic methods employed were scanning electron microscopy (SEM), X-ray photoelectron spectroscopy (XPS), mass loss measurements and residue gas analysis (RGA) during bombardment. Since energetic oxygen bombardment of surfaces may involve a combination of collisional and chemical effects,  $Ne^+$  bombardment representing pure collisional effects was also investigated using the same mass selected ion beam facility.

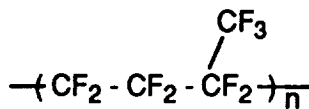
## 2. Experimental

### 2a Targets

Two polymer materials commonly used for space applications were studied, i.e. Kapton H and Teflon FEP supplied by du Pont. The polymers chemical structure is:



KAPTON H



TEFLON FEP

The samples were cleaned prior to bombardment in isopropanol and dried by freon spraying.

## 2b. Irradiation facilities

### The ion beam facility

The main irradiation facility used for the present research was the ion beam facility<sup>(15)</sup> where O<sup>+</sup> and Ne<sup>+</sup> irradiations were carried out (fig. 1). This is a high-output isotope separator operating at a maximum beam energy of 45 keV, to which a beam deceleration stage has been added to produce ions at energies down to 5 eV. For O<sup>+</sup> bombardment, O<sup>+</sup> and other ions are generated in a CO<sub>2</sub> fed discharge ion source. The ions are extracted and accelerated to 20 keV, electromagnetically mass separated and then focused onto a grounded slit before entering the ion deceleration stage. The O<sup>+</sup> ions are then decelerated to an energy E by means of an electrode at a voltage of 20 keV - E. Special care is taken to prevent electrons from being accelerated towards the target. Prior to target bombardment, the O<sup>+</sup> ions are deflected and separated from energetic 20 keV neutrals generated by charge exchange along the beam path. The bombardment is thus of pure, low-energy O<sup>+</sup> ions. A specially designed electron flood gun neutralizes the O<sup>+</sup> charge on insulating targets surfaces. Mechanical rastering is used to achieve uniform irradiations ( $\pm 10\%$  over  $1 \times 1 \text{ cm}^2$ ). The 5eV O<sup>+</sup> flux of this facility was low so that 30eV was selected as a compromise. At this energy the flux was  $10^{15}$  ions/cm<sup>2</sup> sec impinging on a mechanically rastered sample ( $3 \times 1.5 \text{ cm}^2$ ) masked to give an exposed area of  $2 \text{ cm}^2$ . The masked surface was used as a reference for comparison with the bombarded area. The pressure during bombardment was  $10^{-6}$  torr.

### The RF and DC plasma facilities

Two complementary facilities utilized for the present research are a RF plasma system and a DC plasma system. The RF plasma system is a conventional plasma cleaner ("plasma asher") model PDC-3XG manufactured by Harrick Scientific Corporation. This is a 15 watts, 9.3 MHz system with a 25 cm long 7 cm diameter cylindrical chamber. The oxygen plasma is excited at a typical pressure of  $8 \times 10^{-2}$  torr. The thermal energy oxygen plasma composition of plasma ashers has been described in many publications<sup>(2,11-13)</sup>. The DC plasma unit is a home made system where the plasma is generated by a DC discharge between two parallel electrodes. The diameter of the circular electrodes is 10 cm and the distance between the electrodes is 4 cm. The typical working oxygen pressure is  $7 \times 10^{-2}$  torr. The system is pumped by a standard diffusion pump to a pressure of  $10^{-6}$  torr before introduction of the oxygen and starting the DC plasma discharge. A square  $2 \times 2 \text{ cm}^2$  probe is used to detect the plasma current and potential. At typical conditions the current provides a flux of  $5 \times 10^{13}$ - $5 \times 10^{14}$  ions/cm<sup>2</sup> sec with an energy of 30-150 eV depending on the operational conditions. For both plasma systems the fluxes are not uniform and the exact operational conditions are difficult to control and reproduce.

## **2 c. Analyses**

### **Mass loss analysis**

The samples were weighed before irradiation (after being kept at a pressure  $< 2 \times 10^{-6}$  torr for four hours) and after irradiation, by a Mettler UM3 microbalance having a precision of 0.1 $\mu$ g. The bombarded Kapton gained weight during the first minutes of its exposure to atmospheric pressure so that the Kapton measurements were inaccurate within 0.1 mg/cm<sup>2</sup>. The Teflon bombarded samples did not exhibit the same behavior and its weighing accuracy was within  $\pm 10\mu$ g.

### **Residual gas analysis**

Residual gases in the irradiation chamber were monitored by a Dycor M200 quadrupole gas analyzer, manufactured by Ametek. Gas release from the irradiated samples was evaluated by subtraction of the spectra prior to irradiation from those during irradiation.

### **Atomic Force Microscopy (AFM)**

AFM studies were performed under atmospheric pressure using a Digital Instrument Nanoscope II system with two different (15 $\mu$ m and 140 $\mu$ m) scan heads. The surface morphology of the insulating bombarded materials was detected with a sufficient resolution from the 1nm scale without the need of depositing a thin conductive layer (as required for SEM analysis). The evolution of the surface morphology through irradiation by O<sup>+</sup> and Ne<sup>+</sup> fluences of 10<sup>15</sup> ions/cm<sup>2</sup> to 10<sup>19</sup> ions/cm<sup>2</sup> was detected. The surface vertical roughness was measured and statistically averaged by the system.

### **Scanning Electron Microscopy (SEM)**

SEM analysis was performed by a Phillips 525/535 SEM. The analyzed surfaces were coated by a few hundred angstroms of gold to provide good conductivity and high resolution. The SEM images (typically 10 $\mu$ m x 10 $\mu$ m or larger) were compared to the AFM images of the largest scale (also 10 $\mu$ m x 10 $\mu$ m).

### **X-ray Photoelectron Spectroscopy (XPS)**

Bombarded samples were studied by XPS (555 Perkin Elmer system), analyzing the chemical composition of the surfaces. Previous XPS studies<sup>(16)</sup> of irradiated Kapton however indicated its chemical composition changes due to exposure to atmospheric pressure. Another indication to the bombarded Kapton interaction with the atmospheric environment is its weight gain discussed previously.

### 3. Results

#### 3a. Kapton H

##### AFM studies

30 eV  $O^+$  bombardment of Kapton H surfaces using the mass selected ion beam system resulted in significant morphology changes due to surface erosion, (fig. 2). The pristine surface was completely amorphous. Upon successive  $O^+$  bombardment the surface exhibited, in the large scale, a certain roughening and a formation of grain-like features which increased with fluence. Strong changes were also detected in the molecular scale. While the pristine structure exhibited a disordered zigzag pattern with a typical periodicity of about 32Å, a similar analysis performed on top of a grain-like structure in the  $10^{19} O^+/cm^2$  bombarded surface exhibited a smaller periodicity of about 19Å. This latter result may not represent the bombarded surface itself, but reflect its interaction with the ambient atmosphere as previously discussed.

The vertical roughness of pristine and  $O^+$  bombarded surfaces was also investigated (fig. 3). It increased from 10Å for the pristine sample to 0.4  $\mu m$  for the  $10^{19} O^+/cm^2$  bombarded sample. For  $O^+$  fluences smaller than  $5 \times 10^{17} O^+/cm^2$  (low fluence region) the roughness increased very slightly with fluence, while for fluences higher than  $5 \times 10^{17} O^+/cm^2$  (high fluence region) a sharp increase of two orders of magnitude of the surface roughness was observed for a fluence increase of only one order of magnitude. The results of  $O^+$  bombardment were compared to those of  $Ne^+$  bombardment, in order to distinguish between collisional and chemical effects. 30 eV  $10^{19} Ne^+/cm^2$  bombardment of Kapton produces precisely the same roughness as that of 30 eV of  $10^{15} O^+/cm^2$ .

AFM images of Kapton exposed to RF or DC plasmas of oxygen show surface erosion and roughening that increases with fluence. The roughness of RF and DC exposed Kapton is comparable to that of ion beam eroded surfaces for similar mass loss (fig. 4). The exact morphology of samples exposed to the RF and DC oxygen plasmas is different than the morphology following exposure to an  $O^+$  beam. Row-like ordering of the erosion was observed in all heavily eroded samples using the RF and ion beam systems.

##### SEM studies

SEM analysis of the same severely bombarded ( $1 \times 10^{19} O^+/cm^2$ ) Kapton surfaces (fig. 5) displayed porous morphology with needle-like ordering as has been previously reported<sup>(1,9)</sup>. The SEM images reveal the same row-like ordering that was observed by the AFM. It should be noted that using the same magnification, the AFM and SEM images (figs. 4c and 5, respectively) of the same samples are similar. This similarity indicates that the AFM probe did not induce any artifacts in the present results. AFM was however capable of detecting the development of the damage from its initial stage (several nm scale) that could not be detected by the SEM.

## **XPS studies**

XPS studies of both O<sup>+</sup> and Ne<sup>+</sup> bombarded Kapton did not reveal a significant chemical composition change between pristine and bombarded surfaces.

## **Mass Loss Analysis**

The mass loss of Kapton increased linearly with fluence upon O<sup>+</sup> bombardment (fig. 6). The average reaction yield for 30 eV O<sup>+</sup> bombardment was  $3.5 \times 10^{-23} \text{cm}^3/\text{atom}$ . The mass loss upon Ne<sup>+</sup> bombardment was at least one order of magnitude lower than for O<sup>+</sup> irradiation. The accuracy of the mass loss measurements of Kapton is limited ( $\pm 0.1 \text{mg}$ ) due to the interaction between the atmospheric environment and the bombarded sample, and no reliable mass loss of Kapton can be detected for fluences  $< 4 \times 10^{18} \text{O}^+/\text{cm}^2$ .

The mass loss of Kapton exposed to both RF and DC oxygen plasmas increased linearly with the fluence. The reaction yield for the DC plasma exposure can be estimated by assuming that the flux impinging on the sample is equal to the current measured by a probe inserted into the plasma. The reaction yield thus obtained was comparable (slightly lower) to the O<sup>+</sup> beam exposure i.e.,  $1.7 \times 10^{-23} \text{cm}^3/\text{atom}$ . The mass loss rate of Kapton exposed to RF plasma was  $2 \times 10^{-3} \text{mg} \cdot \text{cm}^{-2} \cdot \text{min}^{-1}$ .

### **3b. Teflon FEP**

#### **AFM studies**

AFM studies of pristine and 30 eV O<sup>+</sup> and Ne<sup>+</sup> bombarded Teflon (fluence up to  $10^{19} \text{ions}/\text{cm}^2$ ) were performed. Similar effects were observed for O<sup>+</sup> and Ne<sup>+</sup> bombardment, in contrast to the Kapton bombardment data. The pristine surface structure (Fig. 7a) is built of small features  $\sim 150 \times 150 \text{nm}$  in size, scattered in a chaotic way. The heavily ( $3 \times 10^{18} \text{ions}/\text{cm}^2$ ) bombarded Teflon exhibited a strong surface modification both in the  $\mu\text{m}$  scale and in the nm scale. In the  $\mu\text{m}$  scale (Fig. 7b) the surface is characterized by randomly dispersed hollows ( $\sim 1 \mu\text{m}$  diameter) embedded in a rather smooth area. A higher resolution analysis of these smooth areas reveals a configuration of densely-packed chains 70 nm wide.

AFM images of Teflon exposed to RF and DC plasmas were characterized by a significant nonuniformity of the erosion features. Craters were observed but no  $1 \mu\text{m}$  hollows. The surface roughness of the Teflon eroded by plasmas was higher than the area between hollows for the O<sup>+</sup> exposure.

## **SEM studies**

SEM studies (~20 $\mu\text{m}$  x 20 $\mu\text{m}$  scale) of gold deposited O<sup>+</sup> bombarded Teflon (Fig. 8) reveal eroded surfaces for 3x10<sup>18</sup> ions/cm<sup>2</sup> exposure with ~1  $\mu\text{m}$  holes embedded in a rather smooth matrix similar to that observed by AFM. The roughness of the Ne<sup>+</sup> bombarded surfaces is similar to the O<sup>+</sup> bombarded surfaces, but the morphology of the Ne<sup>+</sup> bombarded Teflon surface looks a little different (the area between the holes is not smooth, but eroded and wrinkled).

## **XPS studies**

XPS analysis of O<sup>+</sup> and Ne<sup>+</sup> bombarded Teflon yielded a strong increase in the C percentage and a corresponding decrease of the F percentage leading to the reduction of the F/C ratio from 2 to 1. A similar phenomenon was reported by others<sup>(6,17)</sup>. The O percentage slightly increased (to 2.6%) following Ne<sup>+</sup> bombardment and more significantly increased (to 8.8%) following O<sup>+</sup> bombardment.

## **Mass Loss analysis**

The mass loss of Teflon also increased with 30 eV O<sup>+</sup> and Ne<sup>+</sup> bombardment fluence (fig. 9). In both cases a reaction yield of ~ 6.5 x10<sup>-22</sup> cm<sup>3</sup>/atom was measured, with no significant difference between O<sup>+</sup> and Ne<sup>+</sup> bombardments.

For both RF and DC oxygen plasmas the mass loss of the exposed Teflon increased with fluence. The mass loss rate of Teflon exposed to RF plasma was 3x10<sup>-3</sup> mg·cm<sup>-2</sup>·min<sup>-1</sup>. The reaction yield of Teflon exposed to DC plasma (assuming that the flux impinging on the sample is equal to the current measured by a probe inserted into the plasma) was 3.2x10<sup>-23</sup> cm<sup>3</sup>/atom, an order of magnitude lower than for 30eV O<sup>+</sup> irradiated Teflon. In both plasma systems the reaction yield of Teflon is higher by a factor of 2 than that of Kapton.

## **RGA analysis**

RGA measurements during 30eV Ne<sup>+</sup> bombardment indicated the release of CF<sub>2</sub> and CF<sub>3</sub>. Similar measurements of 10keV Ne<sup>+</sup> bombardment of Teflon yielded additional peaks, such as C<sub>3</sub>F<sub>3</sub>, C<sub>2</sub>F<sub>4</sub>, C<sub>3</sub>F<sub>4</sub> and C<sub>3</sub>F<sub>5</sub>.

## **4. Discussion**

The ATOX environment in space involves fluxes of neutral 3-7eV atomic oxygen. The main simulation system employed in the present research (the MSIB facility) involves 30eV O<sup>+</sup> ions, and the surface is neutralized by flooding the exposed surface with electrons simultaneously with the 30eV O<sup>+</sup> ions.

The 5eV O<sup>+</sup> flux of this facility was low so that 30eV, (for which a flux of 10<sup>15</sup> O/cm<sup>2</sup> sec and more was obtainable) was selected as a compromise. At this energy, as for higher energies used in many ATOX studies, the bombardment of surfaces with energetic species is associated with several processes occurring in three distinct time scales<sup>(18)</sup>: (i) the collisional stage (~10<sup>-13</sup> sec) where the ions transfer their kinetic energy to target atoms; (ii) the thermalization stage (~10<sup>-11</sup> sec) in which target atoms participating in the collision cascade lose their excess kinetic energy reaching a thermal equilibrium with the surrounding atoms; (iii) the long term relaxation stage (10<sup>-10</sup> sec - 1 sec) in which the final structure of the material is determined and chemical reactions with the residing species may occur. In the collisional stage, the ions lose energy via ionizations, phonon excitations and atomic displacements. In this stage physical sputtering occurs when target atoms are displaced with sufficient energy towards the surface. Surface reconstruction and chemical sputtering are possible during the thermalization stage. Chemical sputtering may be induced by chemical interactions between the bombarding species and the target atoms that form volatile species. Polymer bombardment is more complex than that of inorganic materials since the pure collisional processes (ionizations and atomic displacements) may induce chemical reactions at a later stage due to the formation of radicals, or may initiate cross-linking and scissioning. ATOX simulation facilities may involve species with energies ranging from thermal (< 0.1 eV) to 1 keV. For E < 1 eV the processes are purely chemical and no collisional effects occur. For E = 1 keV the oxygen atom penetrates deep into the polymer (typical range 100Å) creating significant collisional damage along its track and the chemical effect of the oxygen atom trapped at its final position is negligible compared to the collisional effects. For E ~ 5 eV, chemical effects should be dominant but the role of collisional effects must also be determined. Koontz et al.<sup>(2)</sup> have analyzed the reactivity of Kapton to oxygen as a function of the O energy (in the range of 0.05-5 eV) and suggest a purely chemical degradation process that follows an Arrhenius like expression  $R = R_0 \exp(-0.4/E)$  (where R is the mass loss rate and E is the energy) having an activation barrier of 0.4 eV. Ferguson<sup>(14)</sup> performed the same analysis for the energy region of 0.08-800 eV to reach the relation  $R = R_0 E^{0.68}$ . Ferguson's expression can be explained in terms of purely collisional effects where the degradation increases with the energy deposited via collisions.

The Kapton exposure data given in the present work indicates that for 30 eV O<sup>+</sup> bombardment, chemical effects dominate, while collisional effects (determined from Ne<sup>+</sup> bombardment) are smaller by at least one order of magnitude. The reaction yield values obtained in the present work (E = 30 eV) are in accord with earlier published data. Since the Kapton degradation by oxygen in space (E ~ 5 eV) is one order of magnitude lower than our data for E = 30 eV, it follows that in contradiction to the model presented by Koontz et al.<sup>(2)</sup> the chemical degradation by oxygen is energy dependent for 5 eV ≤ E ≤ 30 eV and does not reach a saturation value when exceeding the activation energy of the rate limiting degradation channel. This may be explained by the initiation of additional reaction channels not considered by Koontz et al., or by the increase of the number of target atoms exposed to atomic oxygen following the increase of the O<sup>+</sup> energy. This high reaction yield

value may also be associated with the ionic nature (instead of neutral state in space) of the atomic oxygen used. Another interesting phenomenon associated with Kapton exposure to 30 eV  $O^+$  ions is the nonlinear behaviour of the degradation with  $O^+$  fluence, revealed by the AFM. This behaviour is currently not understood, and may be associated with an increase of the degradation efficiency due to the increase of the bombarded Kapton roughness. The XPS studies indicated that the chemical composition of the bombarded Kapton is very similar to that of the pristine samples. This XPS data may however be misleading since as was previously reported<sup>(23)</sup> the bombarded Kapton is attacked by the ambient atmosphere upon its release from the vacuum chamber, going back to the original Kapton atomic composition. Indeed, the bombarded Kapton samples gain significant weight during their first moments of exposure to the ambient atmosphere. This weight gain may be related to absorption/chemical-interaction processes that occur upon exposure to air.

The Teflon was found to have a different response to 30 eV  $O^+$  and  $Ne^+$  bombardment than Kapton. Since for both ionic species the bombardment of Teflon yields similar mass loss values it can be concluded that for Teflon and 30 eV ion energy, the oxygen degradation is via a collisional process. In accordance to this conclusion, a Teflon FEP bombardment by 750 eV  $Ar^+$  has been reported<sup>(16)</sup> to have a similar reaction yield of  $2 \times 10^{-21} \text{cm}^3/\text{ion}$ . It should be noted that the reaction efficiency of Teflon by 30 eV  $O^+$  is larger by three orders of magnitude than for ATOX in space<sup>(1,2,8)</sup> (20 times larger than Kapton erosion by 30 eV  $O^+$ ). The reason for these high reaction values at  $E = 30 \text{ eV}$  is currently unclear. Residual gas analysis during bombardment indicated the release of  $CF_2$  and  $CF_3$  which was followed by the reduction of the F/C ratio in the bombarded surface from 2 to 1. It thus seems that the energy loss in the collisional process of 30 eV bombardment of Teflon FEP releases very efficiency  $CF_m$  gaseous species, possibly via scissioning.

The erosion processes of Teflon by 5 eV oxygen are still unclear. It is believed<sup>(2)</sup> that Teflon is only very slightly eroded by 5 eV O (reaction yield smaller by a factor of 50 than for Kapton) and that a simultaneous exposure to VUV enhances its reactivity to be similar to that of Kapton. Future experiments by our laboratory will probe the reactivity of Teflon for the whole  $O^+$  range of 5-30 eV in order to understand the sharp increase of reactivity of 3 orders of magnitude in this small energy region.

The previous discussion was focused on the data obtained by the MSIB system. Two additional systems (i.e. RF and DC plasmas) were also used for comparison. The data available from the three systems employed is very much affected by the nature of the three systems. Both plasma systems have a complex nature regarding the species ( $O^+$ ,  $O^+_2$ , excited atoms and molecules, etc.) and the energy spread ( $E < 0.1 \text{ eV}$  for the RF, an unknown distribution of tens up to several hundred eV for the DC plasma). Under such conditions the determination of the flux and the fluence is also difficult. Kapton mass loss serves as a calibration standard, especially for the RF system, while the probe current served as a measure of the flux in the DC system. The comparison between the MSIB data and that of the plasma systems is thus very limited.

For the RF system a comparison of the AFM images can be made for similar mass losses. For Kapton the roughness is similar but the exact surface morphology is different. For Teflon the surface morphology of the eroded surfaces is different, and so is the reaction yield relative to Kapton (~2 for RF and DC and ~20 for MSIB). The actual reaction yields measured using our RF and DC plasma systems are in accord with published data (2,9). The reaction yield of Kapton for the DC plasma is similar to the MSIB but the roughness (for the same mass loss) is much higher. The reaction yield for Teflon is one order of magnitude lower for the DC plasma and the surface morphology is different. It should be noted that the erosion in both plasmas is highly irregular and large variations exist between different tests performed under the same conditions. No such variations were observed for the exposures in the MSIB system. Reaction products of Teflon in different oxygen plasmas were claimed to be responsible for the relatively high reaction yield in these systems (9). This explanation is not applicable for the MSIB system, where relatively higher reaction yields were measured.

The present work has demonstrated that MSIB, where the different physical parameters relevant for erosion studies can be controlled, is capable of elucidation of degradation mechanisms. Specifically it demonstrated that the two commonly used polymers in space applications have entirely different degradation processes for 30eV O<sup>+</sup> exposure. This, along with the comparison to the RF and DC plasmas, indicates that the use of ground ATOX simulation facilities for space materials qualification may lead to erroneous conclusions if the specific erosion mechanisms are not understood.

## **Summary and Conclusions**

The present work can be summarized as follows:

- (i) Chemical processes dominate the degradation of Kapton by 30eV O<sup>+</sup> bombardment.
- (ii) Collisional processes dominate the degradation of Teflon by 30eV O<sup>+</sup> bombardment.
- (iii) Teflon erosion by 30eV O<sup>+</sup> bombardment is 3 orders of magnitude higher than 5eV ATOX erosion in space, indicating different erosion mechanisms for Teflon for these two cases.
- (iv) MSIB offers better control and research possibilities than RF and DC plasmas.
- (v) AFM is an efficient analysis method for the investigation of ATOX erosion from its initial stage to its final stage (1nm-1μm scales).

## **Acknowledgments**

This work was partially supported by the Israel Space Agency (ISA), by the Israel Ministry of Science, and by the Israel Ministry of Absorption. The authors are grateful to Dr. L. Singer of ISA for helpful discussions and support.

## **REFERENCES**

1. L.G.Leger, S.L. Koontz, J.T. Visentine and J.B. Cross, *Proc. of Spacecraft Materials in Space Environment Sympos.*, Toulouse, France, pp. 393-404 (1988).
2. S.L. Koontz, K. Albyn and L.J. Leger, *J. Spacecraft* **28(3)**, 315 (1991).
3. M.R. Reddy, N. Srinivasamurthy and B.L. Agrawal, *ESA Journal* **16**, 193 (1992).
4. K. deGroh, B. Banks, *Proc. of 1st LDEF Post-Retrieval Symposium*, Kissimmee, Florida, June 2-8, 1991.
5. B.A. Banks, S.K. Rutledge, K.K. deGroh, M.J. Mirtich, L. Gebauer, R. Olle and C.M. Hill, *Proc. of 5th Int. Symp. on Materials in a Space Environment*, Cannes-Mandelieu, France, September 16-20, 1991.
6. T.L. Cheeks and A.L. Ruoft, *Mat. Res. Soc. Symp. Proc.* **75**, 527 (1987).
7. R.C. Tennyson, *Can. J. Phys.* **69**, 1190 (1991).
8. W.D. Morison, R.C. Tennyson, J.B. French, T. Braithwaite, M. Moisan and J. Hubert, *Proc. of Spacecraft Materials in Space Environment Sympos.*, Toulouse, France, pp. 435-452 (1988).
9. M. McCargo, R.A. Dammann, T. Cummings and C. Carpenter, *Proc. of Spacecraft Materials in Space Environment Sympos.*, Noordwijk, 1985, ESA SP-232 (1985).
10. K.T. Kern, P.C. Stancil, W.L. Harries, E.R. Long, J. and S.A. Thibeault, *Sample Journal*, **29(3)**, 29 (1993).
11. A.F. Whitaker, B.Z. Jang, *Sampe Journal*, **30(2)**, 30-41 (1994).
12. A.F. Whitaker, B.Z. Jang, *J. Appl. Poly. Sci.* **48**, 1341-1367 (1993).
13. T. Wydeven, M.A. Golud, N.R. Lerner, *J. Appl. Poly. Sci.*, **37**, 3343-3355 (1989).
14. D.C. Ferguson, *Proc. of the 13th Space Simulation Conference*, Orlando, FL, 1984, CP-2340, 205 (1984).
15. I. Chavet, M. Kanter, I. Levy, H.Z. Sar-El, *Proc. 8th Int. EMIS Conf.*, Skovde, Sweden (Institute of Physics, Sweden, p. 191 (1973).
16. K.S. Sengupta and H.K. Birnbaum, *J. Vac. Technol. A.* **9(6)**, 2928 (1991).
17. H.B. Gjerde, T.R. Chun, S.J. Low, *Proc. of the 18th International SAMPE Technical Conference, 1986*, 262, (1986).
18. B.W. Dodson in *Material Research Society Symposium Proceeding (MRC, Pittsburgh, 1989)*. **128**, 127 (1989).
19. J.S. Sovey, *J. Vac. Sci. Technol.* **16(2)**, 813 (1979).

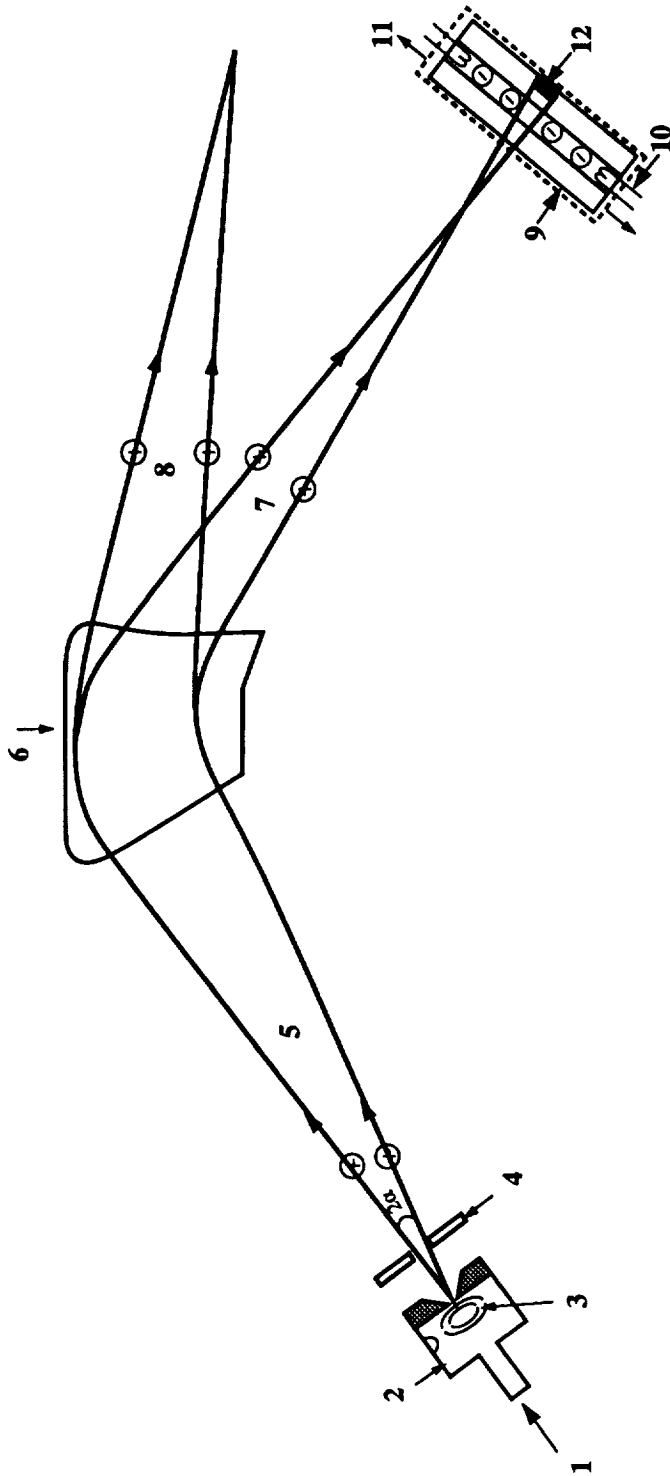


Fig. 1 - Schematic view of the mass selected ion beam facility: 1. CO<sub>2</sub> or Ne Gas inlet, 2. Ion source, 3. Electric arc, 4. Acceleration electrode, 5. High energy C<sup>+</sup>, O<sup>+</sup>, CO<sup>+</sup>, CO<sub>2</sub><sup>+</sup>, ions, 6. Separation magnet, 7. O<sup>+</sup> or Ne<sup>+</sup>, 8. C<sup>+</sup>, CO<sup>+</sup>, CO<sub>2</sub><sup>+</sup>, 9. Deceleration assembly, 10. Surface charge neutralization, 11. Mechanical scanning assembly, 12. Substrate

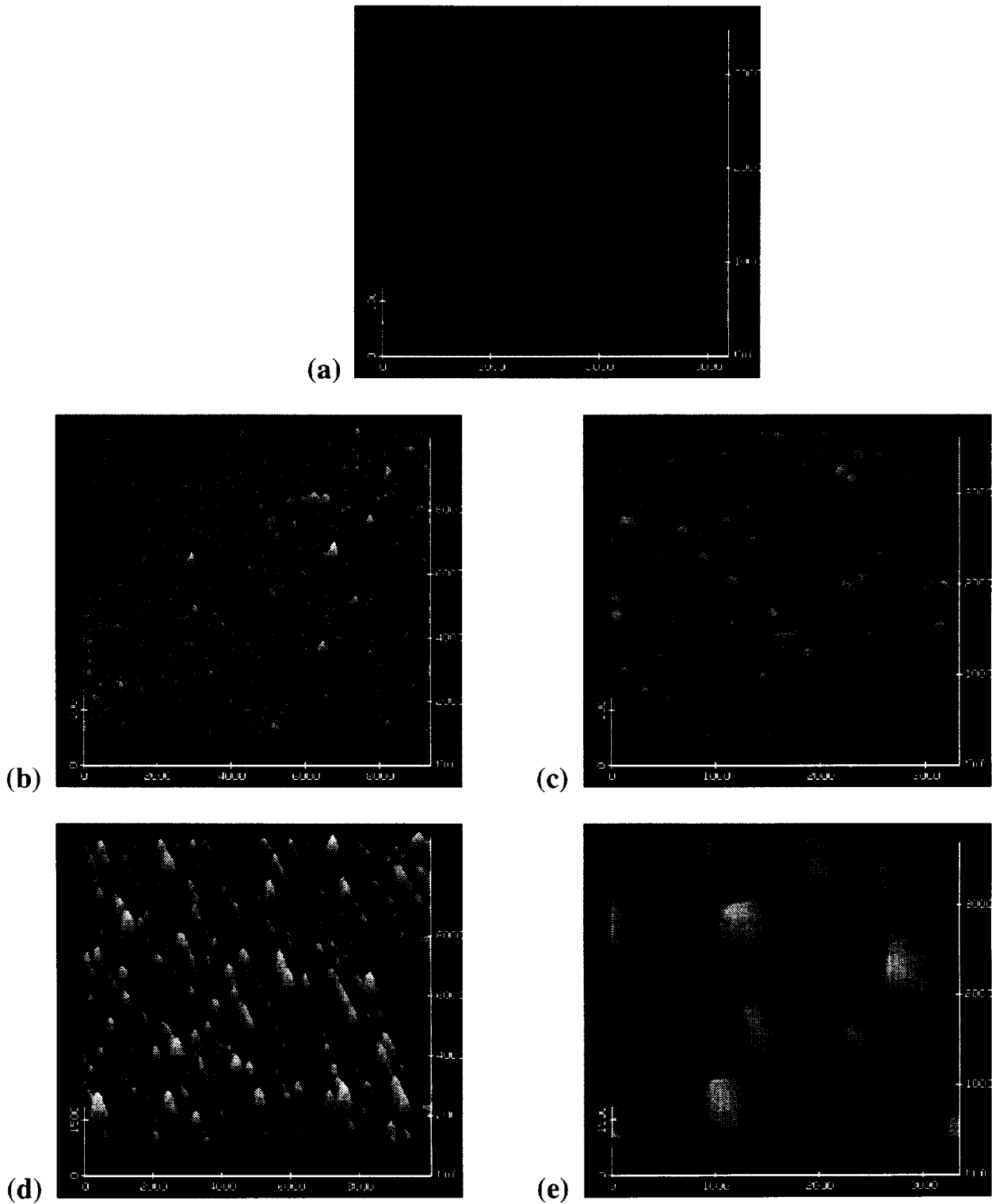


Fig. 2 - AFM images Kapton at different stages of 30 eV  $O^+$  bombardment. (a) Pristine. (b)  $10 \mu\text{m} \times 10 \mu\text{m}$  and (c)  $3.3 \mu\text{m} \times 3.3 \mu\text{m}$  -  $O^+$  flux of  $5 \times 10^{17}$  ions/cm<sup>2</sup> (d)  $10 \mu\text{m} \times 10 \mu\text{m}$  and (e)  $3.3 \mu\text{m} \times 3.3 \mu\text{m}$  -  $O^+$  flux of  $1 \times 10^{19}$  ions/cm<sup>2</sup> Note the different z scales: 100 nm for (a), (b) and (c), and 1500 nm for (d) and (e).

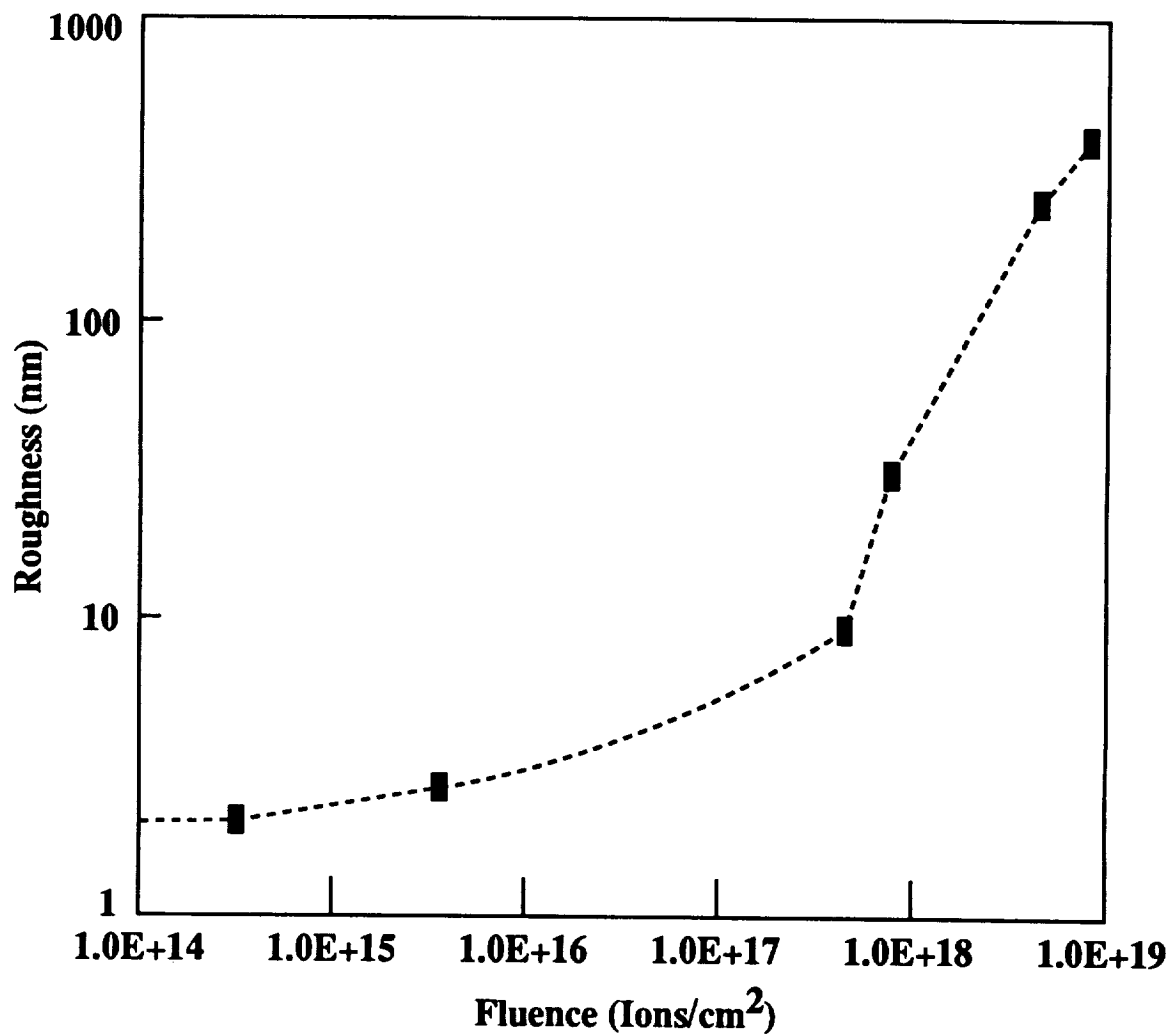


Fig. 3 - The vertical roughness of 30 eV O<sup>+</sup> bombarded Kapton surfaces (studied by AFM) as a function of fluence.

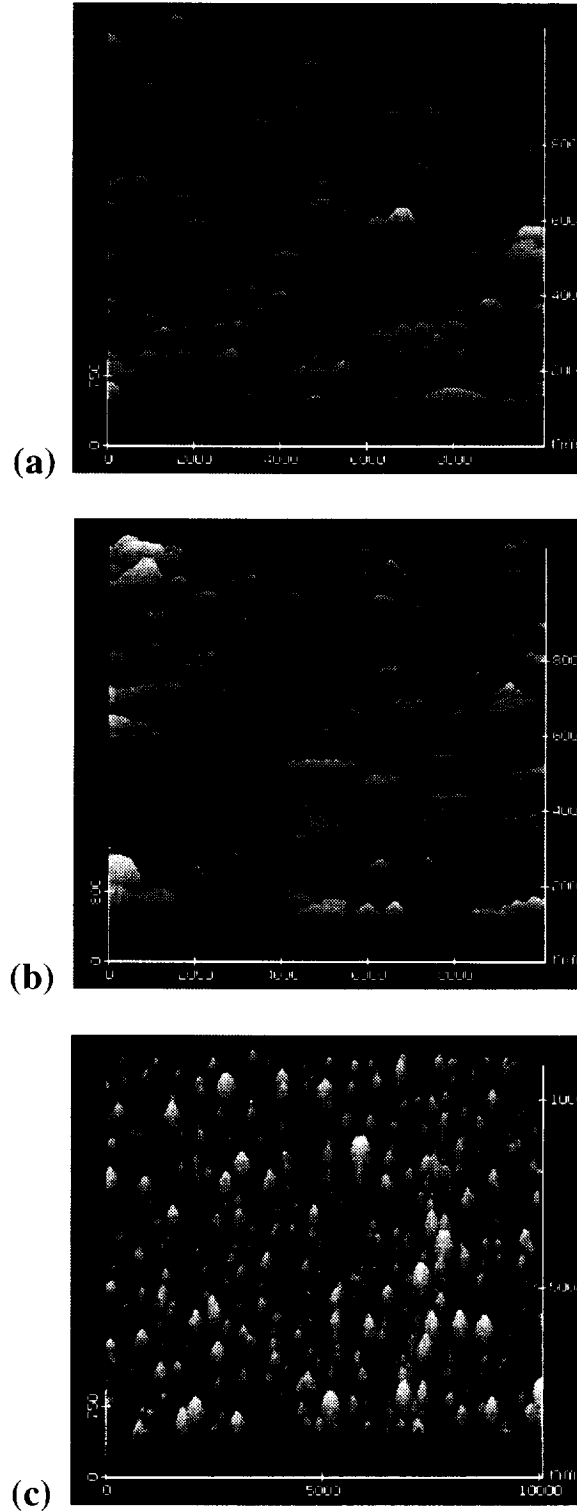


Fig. 4 - AFM images ( $10 \mu\text{m} \times 10 \mu\text{m}$ ) of Kapton exposed to oxygen with a similar mass loss of  $0.2 \text{ mg}/\text{cm}^2$  (a) DC plasma, fluence of  $5 \times 10^{18} \text{ O}^+/\text{cm}^2$ ; (b) RF plasma, fluence of  $5 \times 10^{20} \text{ O}^+/\text{cm}^2$ ;

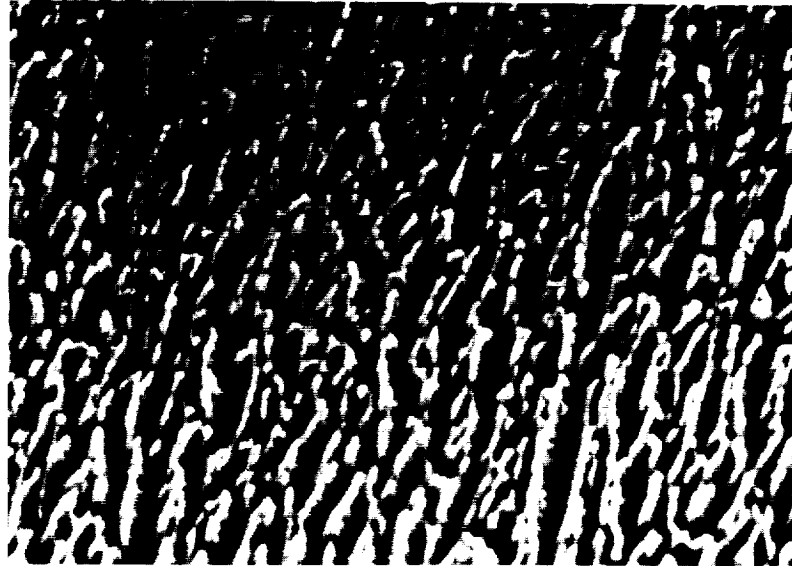


Fig. 5 - SEM image (10 $\mu$ m x 10 $\mu$ m) of a Kapton surface eroded by 30 eV O<sup>+</sup> at a fluence of  $1 \times 10^{19}$  ions/cm<sup>2</sup>.

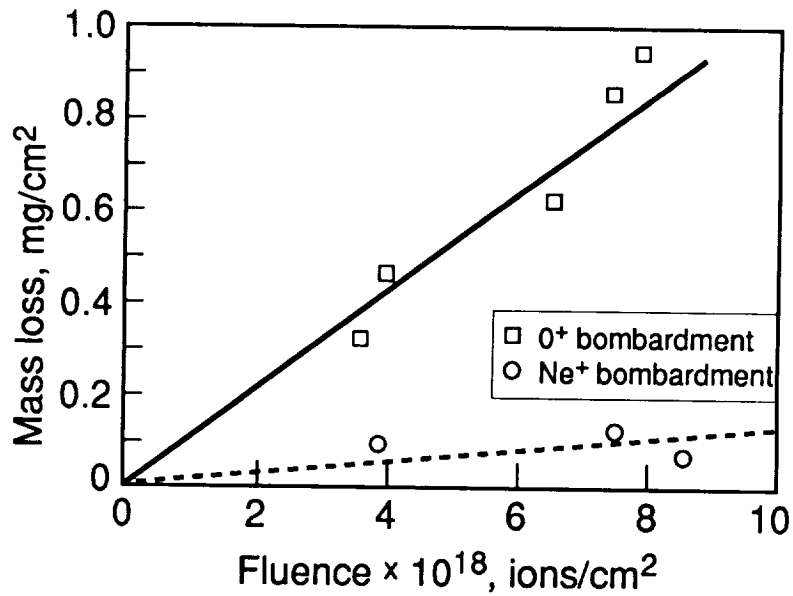


fig. 6 - The mass loss of Kapton surfaces as a function of fluence at 30 eV O<sup>+</sup> and Ne<sup>+</sup>.

Note: (i) significant erosion by O<sup>+</sup>, small erosion by Ne<sup>+</sup>; (ii) the Kapton eroded surfaces gained weight upon exposure to atmospheric pressure leading to an inaccuracy of 0.1 mg in the measurements.

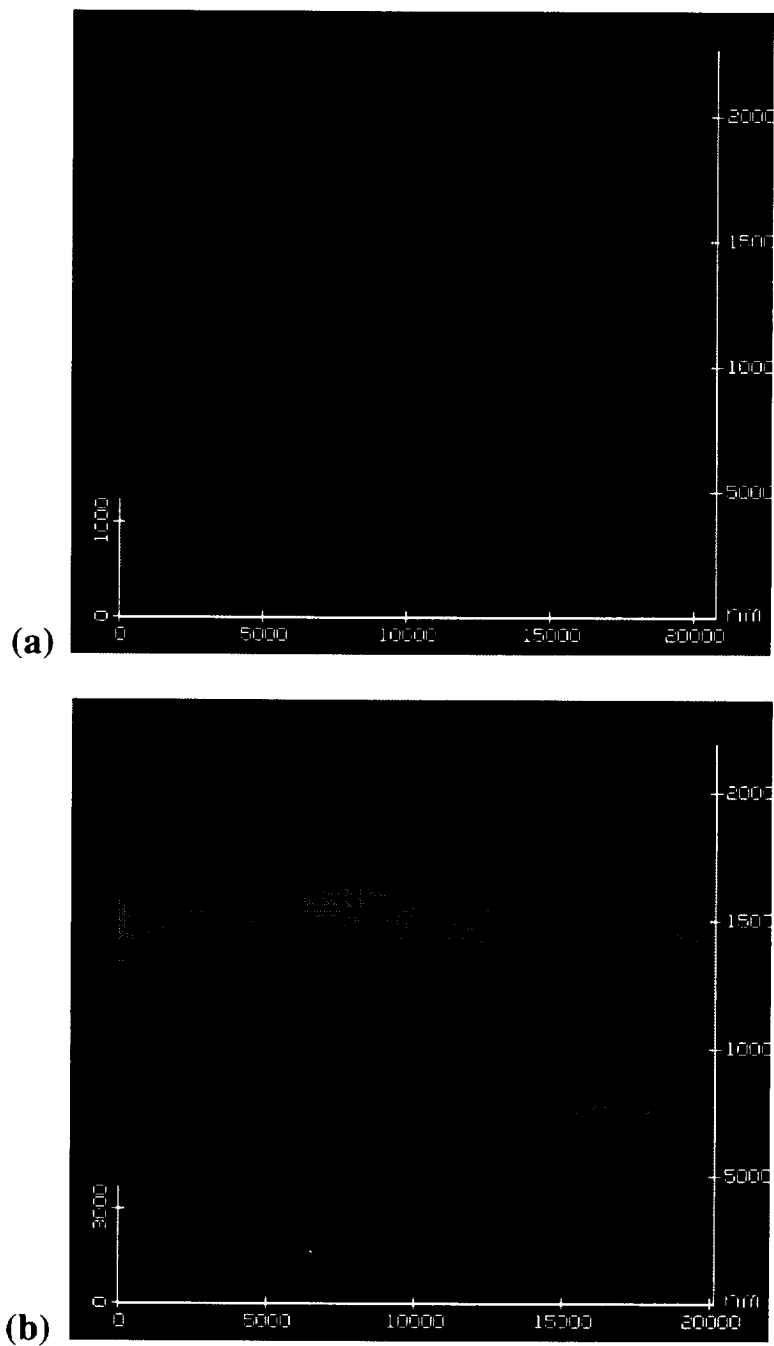


Fig. 7 - AFM images ( $20\ \mu\text{m} \times 20\ \mu\text{m}$ ) of Teflon. (a) pristine; (b) after  $30\ \text{eV}\ \text{O}^+$  bombardment at a fluence of  $3 \times 10^{18}$  ions/ $\text{cm}^2$ ;  
Note the different z scale,  $1000\ \text{nm}$  for (a) and  $3000\ \text{nm}$  for (b).

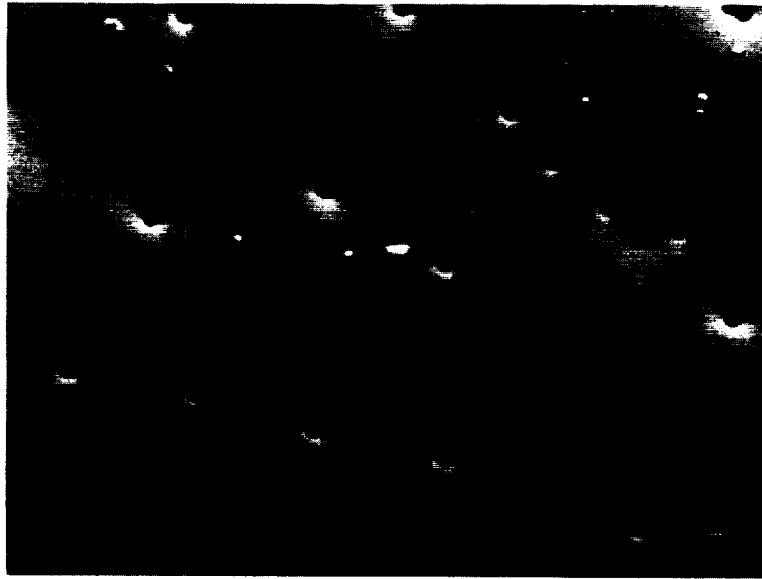


Fig. 8 - SEM image ( $20\mu\text{m}\times 20\mu\text{m}$ ) of Teflon eroded by 30 eV  $\text{O}^+$  ions at a fluence of  $3 \times 10^{18}$  ions/ $\text{cm}^2$ .

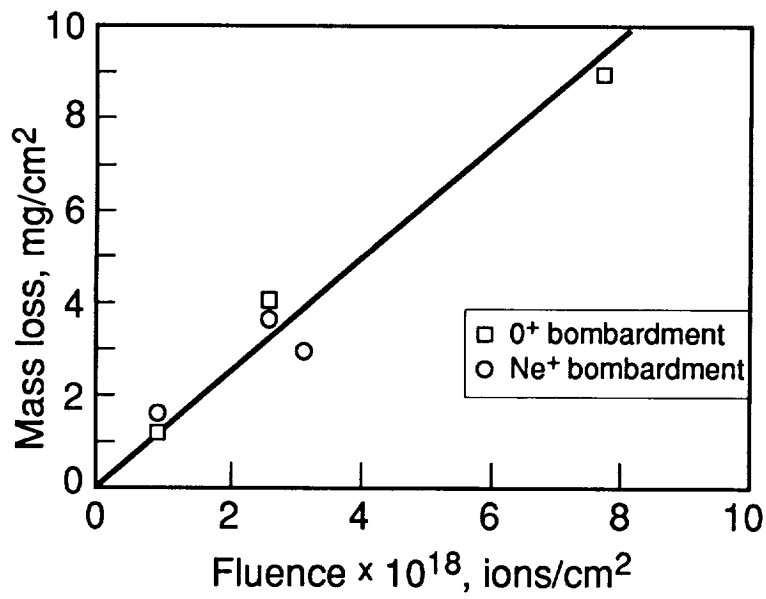


Fig. 9 - The mass loss of Teflon surfaces as a function of fluence at 30 eV  $\text{O}^+$  and  $\text{Ne}^+$  bombardment.

Note: similar erosion by  $\text{O}^+$  and  $\text{Ne}^+$ .